Mechanics-based statistics of failure risk of quasibrittle structures and size effect on safety factors

Zdeněk P. Bažant* and Sze-Dai Pang†

Department of Civil Engineering and Materials Science, Northwestern University, Evanston, IL 60208

Contributed by Zdeněk P. Bažant, April 4, 2006

In mechanical design as well as protection from various natural hazards, one must ensure an extremely low failure probability such as 10^{-6}. How to achieve that goal is adequately understood only for the limiting cases of brittle or ductile structures. Here we present a theory to do that for the transitional class of quasibrittle structures, having brittle constituents and characterized by nonnegligible size of material inhomogeneities. We show that the probability distribution of strength of the representative volume element of material is governed by the Maxwell–Boltzmann distribution of atomic energies and the stress dependence of activation energy barriers; that it is statistically modeled by a hierarchy of series and parallel couplings; and that it consists of a broad Gaussian core having a grafted far-left power-law tail with zero threshold and amplitude depending on temperature and load duration. With increasing structure size, the Gaussian core shrinks and Weibull tail expands according to the weakest-link model for a finite chain of representative volume elements. The model captures experimentally observed deviations of the strength distribution from Weibull distribution and of the mean strength scaling law from a power law. These deviations can be exploited for verification and calibration. The proposed theory will increase the safety of concrete structures, composite parts of aircraft or ships, microelectronic components, microelectromechanical systems, prosthetic devices, etc. It also will improve protection against hazards such as landslides, avalanches, ice breaks, and rock or soil failures.

cohesive fracture | extreme value statistics | activation energy | Maxwell–Boltzmann | scaling

Engineering structures must be designed for extremely low failure probability (1, 2), such as $P_f = 10^{-6}$ to 10^{-7}. If the typical probability density function (pdf) of the applied load is taken into account, the pdf of structural strength need not be known for all $P_f > 10^{-6}$ to 10^{-7}, but it must still be known for all P_f greater than $\approx 10^{-5}$ to 10^{-6}. Very low P_f also is required in microelectronics, microelectromechanical systems (MEMS), biomedical devices, and in protection from various natural hazards. For such low P_f, direct determination of the tail of the pdf of failure load F from experimental histograms is virtually impossible. Therefore, one must rely on a theory to be verified indirectly. Its formulation has been a fundamental problem of failure mechanics, in which only two limiting failure types are now adequately understood (3): (*i*) perfectly ductile (plastic) failures, where F is essentially a weighted sum of the strength contributions from all the representative volume elements (RVEs) of the material lying on the failure surface, and (because of the central limit theorem of probability) the pdf of F is necessarily Gaussian, or normal (except in far-left tails); and (*ii*) perfectly brittle failures, which are decided by the failure of one RVE and thus follow the weakest-link model, leading to Weibull pdf. In these limit cases, encompassing classical, monotonically loaded, or fatigued metallic structures, the confidence in the estimation of load of extremely low P_f is high because the pdf is theoretically well justified and is independent of structure size and geometry.

Here we show how to solve the problem, including its scaling aspect, for the broad and increasingly important class of quasibrittle structures, the failure behavior of which lies between these two extremes (for the details, mathematical derivations, and computations, see ref. 4). Although the material constituents of such structures are brittle, a heterogeneous microstructure causes the RVE not to be negligible compared with the characteristic size D (or cross-section dimension) of the structure. This category includes most structures or bodies consisting of concrete, rock, stiff soils, sea ice, consolidated snow and wood, as well as modern "high-tech" materials such as toughened ceramics, fiber composites, and rigid foams, or biological materials such as bone, cartilage, tooth enamel, dentin, or sea shells. Because every brittle structure becomes quasibrittle when scaled down to $D < \approx 1{,}000 l_0$, where l_0 is RVE size, the problem will be important for materials on the nanometer and micrometer scales (e.g., nanocomposites, MEMS, and thin films).

Attention will be restricted to structures of positive geometry: a typical and dangerous case in which the removal of one RVE at constant load causes instability and dynamic failure (5). When $D/l_0 \to \infty$, the geometry is positive if the partial derivative of the stress intensity factor with respect to the crack length is positive, and approximately this criterion is used for any D.

According to the classical statistical theory of brittle failure (6), a structure of positive geometry fails as soon as the random material strength is reached at one point of the structure. Quasibrittle structures of positive geometry, in which the RVE size is not negligible, fail when the strength of one RVE as a whole is exhausted. In other words, a weakest-link statistical model with finite number, N, of links in a chain must be used. The RVE is defined here as the smallest element whose failure will cause the whole structure to fail [the homogenization theory is inapplicable because it captures only low-order statistical moments and misses the far-out cumulative probability density distribution function (cdf) tail of RVE, which totally controls the strength of large structures]. Typically, the RVE size, l_0, is approximately double or triple the maximum inhomogeneity size (or grain size).

Tail Distribution of Strength on Nanoscale

The existing micromechanical justification of the Weibull theory of statistical strength in terms of the distribution of material

Conflict of interest statement: No conflicts declared.

Abbreviations: pdf, probability distribution function; cdf, cumulative probability density distribution function; RVE, representative volume element; MEMS, microelectromechanical systems.

*To whom correspondence should be addressed at: McCormick School of Engineering and Applied Science, Northwestern University, 2145 Sheridan Road, CEE, Evanston, IL 60208. E-mail: z-bazant@northwestern.edu.

†Present address: Engineering Science Program and Civil Engineering Department, National University of Singapore, Singapore 117576.

www.pnas.org/cgi/doi/10.1073/pnas.0602684103

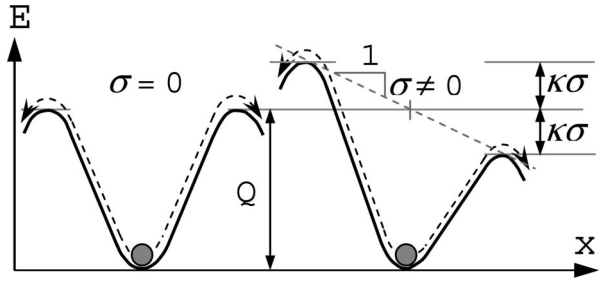

Fig. 1. Interatomic potential profile and change of activation energy barrier caused by applied stress σ.

flaws (7, 8) involves hypotheses hardly better justified than the macroscopic theory itself. Here we propose to base the theory on the severance of interatomic bonds. According to the Maxwell–Boltzmann distribution of thermal energies of atoms (9–12), the frequency of severance of bonds is $\exp[-(Q - \kappa\sigma)/kT]$, and the frequency of bond restorations is $\exp[-(Q + \kappa\sigma)/kT]$, where T is absolute temperature, Q is activation energy, κ is a constant coefficient (13), and k is the Boltzmann constant (Fig. 1).

Hence, the net frequency, f_b, of permanent bond breaks is $\exp[-(Q - \kappa\sigma)/kT] - \exp[-(Q + \kappa\sigma)/kT] = 2\exp(-Q/kT)\sinh(\kappa\sigma/kT)$. A contiguous nanocrack on the atomic scale may be considered to form when the accumulated number of broken bonds reaches a certain threshold (in the sense of percolation theory). The load duration, τ, needed for that to happen is proportional to $1/f_b$. Therefore, the cdf of creating a contiguous nanocrack must have the form $F(\sigma) = \min[C_0\tau\exp(-Q/kT)\sinh(\kappa\sigma/kT), 1]$ (for $\sigma \geq 0$), where C_0 is the empirical constant. Hence

$$F(\sigma) \approx C_b\sigma, \quad C_b = C_0\frac{\kappa}{kT}\tau e^{-Q/kT} \quad \text{for } \sigma \to 0. \qquad [1]$$

So, the cdf of strength of a nanoconnection has a power-law tail with exponent 1 and threshold 0. This point is essential.

Strength Distribution of One RVE

The size of RVE of a quasibrittle material such as concrete, with the maximum mineral grain size of ≈2 cm, is separated from the atomic lattice by a scale spanning 8 orders of magnitude. The failure of RVE may involve damage such as microcracking at all these scales. Their bridging must, from the probabilistic viewpoint, be represented as some combination of series and parallel couplings of elements of random strength. The tail of cdf is particularly important.

The weakest-link, or series coupling, model (Fig. 2*b*) is the simpler case. If all of the elements (links of a chain) have a cdf with power-law tail $P_f = (\sigma/s_1)^p$ of exponent p (and scale parameter s_1), reaching (with a fixed error such as 1%) up to failure probability $P_{t_1} = (t_1/s_1)^p$, then the chain of n links has a power-law tail of the same exponent p, reaching up to failure probability P_{t_n} that ensues from the condition of joint probability of survival of all links

$$P_{t_n} = 1 - \left(1 - \frac{t_1^p}{s_1^p}\right)^n \underset{n\to\infty}{\Rightarrow} 1 - e^{-n(t_1/s_1)^p} \underset{t_1\to 0}{\Rightarrow} \frac{nt_1^p}{s_1^p} = nP_{t_1}. \qquad [2]$$

The failure probability up to which P_f is a power law increases in proportion to the number, n, of elements, as long as P_{f_t} is sufficiently small, whereas afterward the cdf converges to the Weibull cdf (see Eq. **2**). If, e.g., the tail of the cdf of one RVE is a power law for $P_f < 0.0005$ with a 1% error (the cdf for $P_f >$ 0.0005 being arbitrary), then a chain of 100 RVEs has a power-law tail for $P_f < 0.05$ with a 1% error, and a chain of 10,000 RVEs has a Weibull cdf (except for $P_f \geq 0.993$).

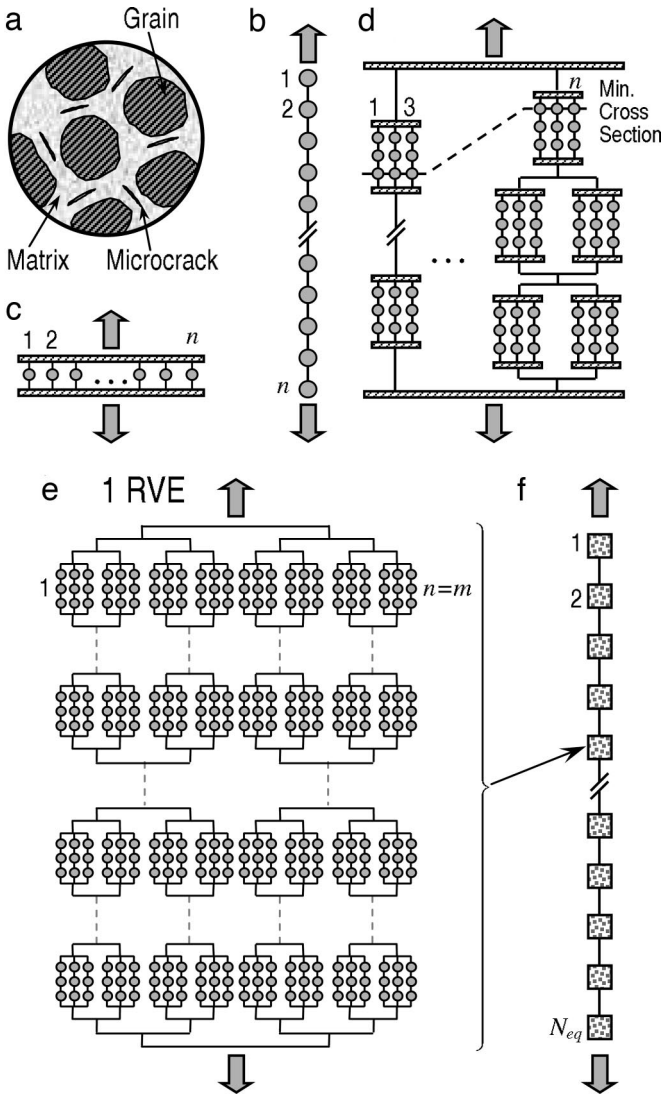

Fig. 2. Models for extreme-value statistics of strength. (*a*) Potential break surfaces within a connection layer between hard inclusions, representing a RVE. (*b*) Chain model. (*c*) Fiber bundle model. (*d*) Example of statistical model of RVE with subchains and subbundles. (*e*) Hierarchy of subchains and subbundles. (*f*) A weakest-link model made up of elements, each representing one RVE.

In the case of parallel coupling (or the "fiber bundle" model) (Fig. 2*c*), one must distinguish brittle and plastic elements (usually called "fibers"). Brittle elements are those for which the stress drops to 0 as soon as the peak stress (or strength) of the element is reached, and plastic ones are those for which the stress remains constant at continuing deformation. The real behavior surely consists of gradual postpeak softening, which is hard to handle analytically but may be expected to be bounded by the brittle and plastic behaviors.

For brittle fibers, the cdf of the strength σ of a bundle ensues from the recursive equation of Daniels (14), giving the cdf $G_n(\sigma)$ for a bundle of n fibers in terms of $G_{n-1}(\sigma)$ for a bundle of $n - 1$ fibers. As shown by Daniels, $G_n(\sigma)$ converges, for $n \to \infty$, to the error function (Gaussian cdf) regardless of the cdf of individual brittle fibers. The same is obviously true for plastic fibers, as indicated by the central limit theorem (15).

ENGINEERING

If the tail of one-fiber cdf is $\approx\sigma^p$, then the tail of $G_n(\sigma) \propto \sigma^{np}$ for both brittle and plastic fibers (and likely also for the intermediate case of softening fibers). Therefore, the tail exponents in a bundle are additive. For brittle fibers, this finding can be proven by induction from set theory (16) or by series expansion of $G_n(\sigma)$ in terms of powers of σ (ref. 4; see also refs. 17–19). For plastic fibers, this property follows by induction from additivity of tail exponents p and q in a bundle of two fibers with tails σ^p and σ^q [which ensues, e.g., by Laplace transform, from the convolution integral for pdf of a sum (4)].

Length of Power-Law Tail

The reach of the power-law tail of cdf of a bundle shrinks rapidly with increasing n. Introducing power series expansions of pdf into Daniel's recursive equation for the brittle case, or into the convolution integral for the plastic case, one can show (4) that the reach of the power-law tail in terms of failure probability decreases with the number n of fibers rapidly as $P_{t_n} \sim (P_{t_1}/n)^n - (P_{t_1}/3n)^n$ if brittle, or $(P_{t_1}/n)^n$ if plastic.

Thus, it is found that if the cdf of strength of a RVE of a material having Weibull modulus $m = 24$ were represented as a bundle of fibers with power tails reaching up to $P_f = 0.003$, then for 2, 3, 6, and 24 parallel fibers (whose tails must have exponents 12, 8, 4, and 1) the power-law tail of the bundle terminates at 5.5×10^{-5}, 1.3×10^{-7}, 3.8×10^{-13}, and 3.6×10^{-45} for brittle fibers or at 3.0×10^{-3}, 7.2×10^{-5}, 3.0×10^{-9}, and 7.2×10^{-44} for plastic fibers, respectively (4). Therefore, we must conclude that if the RVE were modeled by more than two or three elements, the power-law tail would be so short that structures behaving as a chain of RVEs could never exhibit a Weibull cdf. The fact that they do implies that a model for extreme value statistics of one RVE of quasibrittle material cannot include more than two or three elements coupled in parallel. It also transpires that, for plastic (or ductile) materials, the RVE model must involve parallel couplings with $\geq$4 elements, to push the power-law tail so far left that Weibull pdf could not develop for any realistic structure size.

Note also that if a significant part or the whole of strength distribution of one alleged RVE of quasibrittle material were Weibull, this alleged RVE could not really be a RVE because it would have to behave as a chain in which failure must localize into one link having very short power-law tail. This link would be the true RVE, smaller than the alleged RVE. For the same reason, the topmost coupling must be a parallel coupling, or else the actual RVE would be smaller than alleged.

Physical Meaning of Weibull Modulus

In the idealized statistical model of Fig. 2*e*, as well as irregular hierarchical models of Fig. 2*d*, the tail exponent of RVE, i.e., the Weibull modulus m, represents the number of connections that must be severed to separate the model into two halves. These highest-scale connections may be imagined to correspond to the number dominant cracks that are required to break a RVE (Fig. 2*a*). This number, in turn, depends on the packing of inhomogeneities (or grains) in the RVE. Therefore, the packing appears to be what physically determines the value of Weibull modulus.

Structure as a Chain of RVEs

Consequently, the model, idealized in Fig. 2*e*, must be hierarchical, consisting of parallel and series couplings. It consists of a bundle of two long subchains, each of which consists of two subbundles of two long sub-subchains of sub-subbundles, etc., until the nanoscale connections whose cdf has the tail σ^1 is reached. The first parallel coupling raises the tail exponent of 1 to 3, the next to 6, the next to 12, and the last to 24, while each such coupling drastically shortens the power-law tail. The shortening is offset, at each level of hierarchy, by a long enough chain, lengthening the power-law tail.

Based on the stress effect on the activation energy of bonds governed by Maxwell–Boltzmann distribution, the idealized model in Fig. 2*e* can produce, for one RVE, a cdf with two essential characteristics: (*i*) a power-law tail whose exponent m is $\approx$10–50, typical of Weibull moduli observed for various brittle materials, and (*ii*) a power-law tail reaching to $P_f = 0.0001$ to 0.01, which is a chain of 100–10,000 RVEs. For such sizes or larger, laboratory specimens of heterogeneous brittle materials follow the Weibull cdf (6, 20–28), whereas the behavior of the smallest possible test specimens of such materials can be described as Gaussian (29–33) (except for the far-left tail of histograms of strength tests that is normally undetectable).

When the stress field is nonuniform, the weakest-link model for structural failure must be based not on the actual number N of RVEs in the structure but on the equivalent number of RVEs, N_{eq}. If the cdf tail of one RVE of size l_0 is $P_1 = (\sigma_N/s_0)^m$, then, according to the classical Weibull theory, $P_f = 1 - \exp[-(\sigma_N/S_0)^m]$, where $S_0 = s_0(l_0/D)^{n_d/m\Psi - 1/m}$ and $\Psi = \int_V[\bar{\sigma}(\xi)]^m \mathrm{d}V(\xi)$ is a geometry parameter independent of D; n_d is the number of dimensions in which the failure is scaled; V is structure volume; $\xi = x/D$ is the dimensionless coordinate vector; x is the coordinate vector of material points; $\sigma_N = F/bD$ or F/D^2 is the nominal stress or load parameter of the dimension of stress (where b is structure thickness); m is the Weibull modulus; s_0 is the scaling parameter of power-law tail (measured on a specimen of one RVE's size); $\bar{\sigma} = \sigma(x)/\sigma_N$; and σ is the positive part of the maximum principal stress at x, which depends on structure geometry but not on D if geometrically similar structures are considered. According to Eq. **1**

$$s_0 = s_{0r}(T\tau_0 / T_0\tau)e^{(T^{-1}-T_0^{-1})Q/k}, \qquad [3]$$

where T_0, τ_0, and s_{0r} are the values of T, τ, and s_0 in chosen reference conditions.

For a structure with large enough N_{eq}, the foregoing expression for P_f must coincide with $P_f = 1 - \exp[-N_{eq}(\sigma_N/s_0)^m]$. This condition furnishes

$$N_{eq} = (s_0 / S_0)^m = (D/l_0)^{n_d}\psi. \qquad [4]$$

The geometry factor Ψ is assumed to apply not only for large N_{eq} but approximately also for small N_{eq}, for which the deviation from Weibull cdf is significant.

Applying the joint probability theorem to a chain yields

$$P_f(\sigma_N) \underset{\text{any } N_{eq}}{=} 1 - [1 - P_1(\sigma_N)]^{N_{eq}} \underset{N_{eq}\to\infty}{\Rightarrow} 1 - e^{N_{eq}(\sigma_N/s_0)^m}, \qquad [5]$$

where $P_1(\sigma_N)$ is the cdf of strength of one RVE. The corresponding pdf is $p_1(\sigma_N) = \mathrm{d}P_1(\sigma_N)/\mathrm{d}\sigma_N$. According to Eq. **3**, the scale parameter s_0 captures the dependence of cdf on temperature and loading rate or duration.

Grafted Probability Distribution for One RVE

Although the transition of $p_1(\sigma_N)$ from Weibull pdf to Gaussian pdf ought to gradual, for the sake of simplicity we may consider that a Weibull pdf $\phi_W(\sigma_N)$ is grafted from the left onto a Gaussian pdf $\phi_G(\sigma_N)$

$$p_1(\sigma_N) = r_f\phi_W(\sigma_N), \quad \text{for } \sigma_N < \sigma_{N,gr}; \qquad [6]$$

$$= r_f\phi_G(\sigma_N), \quad \text{for } \sigma_N \geq \sigma_{N,gr}, \qquad [7]$$

where $\phi_W(\sigma_N) = (m/s_1)(\sigma_N/s_1)^{m-1}\exp[-(\sigma_N/s_1)^m]$; $\phi_G(\sigma_N) = \exp[-(\sigma_N - \mu_G)^2/2\delta_G^2]/(\delta_G\sqrt{2\pi})$; here μ_G and δ_G are the mean and standard deviation of the Gaussian part, and m and s_1 are

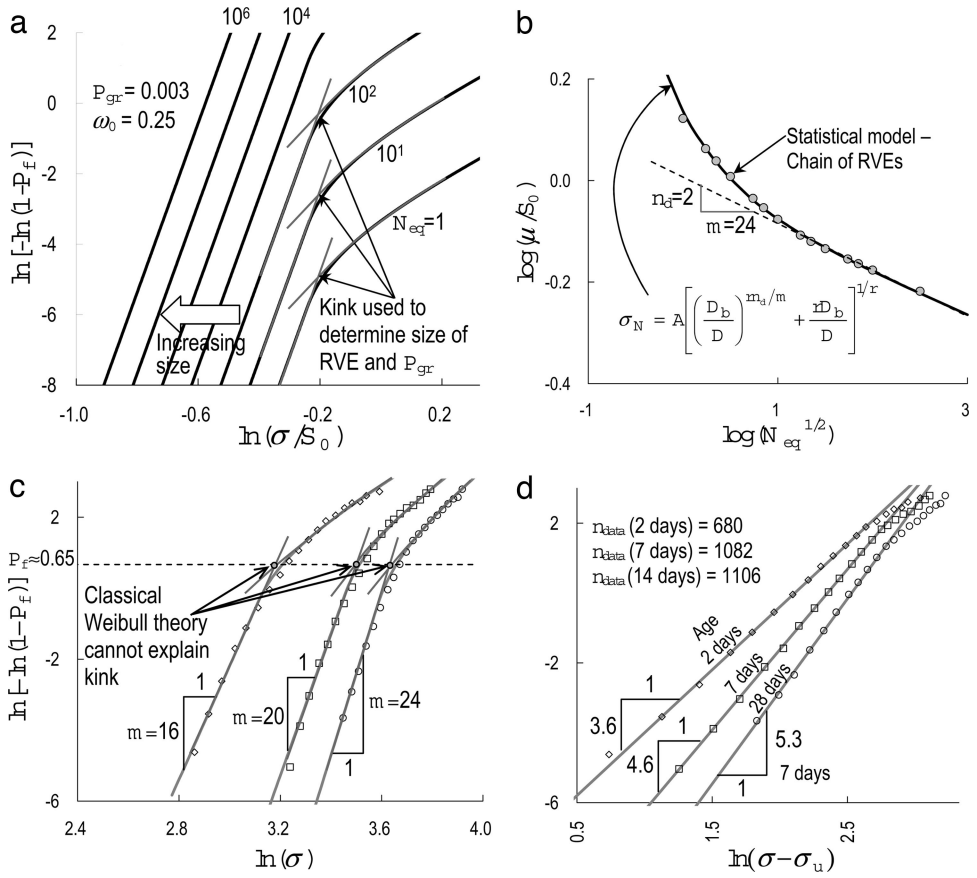

Fig. 3. Effects of structure size. (*a*) Size effect on the cdf of structural strength for $P_{gr} = 0.003$, $\omega_0 = 0.25$ in Weibull scale. (*b*) Optimum fits of chain-of-RVEs model by asymptotic matching size effect formula (35) (*A*, D_b, *r* = fitting constants). (*c*) Weibull's (1939) tests (6) of Portland cement mortar of age 2, 7, and 28 days, and fits by the present chain-of-RVEs model, with zero threshold. (*d*) The same tests as originally fitted by Weibull distribution with finite threshold.

the shape and scale parameters of the Weibull part. The far-left power tail of P_1 may be related to s_1

$$\text{for } \sigma_N \to 0: \quad P_1 = (\sigma_N/s_0)^m, \quad s_0 = r_f^{1/m} s_1. \qquad [8]$$

The continuity condition of pdf at the grafting point requires $\phi_W(\sigma_N) = \phi_G(\sigma_N)$, i.e., equality of Eqs. **6** and **7**, for $\sigma_N = \sigma_{N_{gr}}$. The scaling factor r_f must ensure that $\int_{-\infty}^{\infty} \phi(\sigma_N)d\sigma_N = 1$. This normalizing condition, the continuity condition, Eq. **8**, and the pdf expression given by Eqs. **6** and **7** (with s_0 and s_1 related by Eq. **8**) amount to four conditions, from which r_f, μ_G, δ_G, and P_{gr} (or $\sigma_{N_{gr}}$) can be calculated if the values of m, s_0 (or s_1), overall mean μ, and overall coefficient of variation $\omega = \delta/\mu$ are known.

Verification and Calibration

Although for $N_{eq} = 1$ (one RVE, $D = l_0$), the cdf slope is at the grafting point discontinuous, for $N_{eq} > 1$, Eq. **5** gives a continuous slope everywhere. For finite but not too large N_{eq}, the lower part of cdf appears as a straight line on the Weibull probability paper, whereas the upper, Gaussian, part appears curved (Fig. 3*a*). The upper part of cdf appears as a straight line on the normal (Gaussian) probability paper, whereas the lower, Weibull, part appears curved. These two straight lines can be identified in the proper probability papers by linear regression of the lower and upper parts of the histogram of structural strength data for a certain fixed D (or N_{eq}). These parts intersect at a point, called the kink point, which represents the center of the transition from Weibull to Gaussian cdf. With increasing structure size, the kink point moves upward, from the lower extreme to the upper extreme of the cdf (Fig. 3*a*). Experimental observations of the kink point for various structure sizes and shapes provide one way to verify and calibrate the theory.

Consider that the kink points (σ_{N_i}, P_{f_i}) [1 = 1, 2, . . . , n_k (Fig. 3*a*)] have been identified for a number of different sizes N_{eq_i} corresponding to different sizes D_i and geometry parameters Ψ_i. Eq. **5** must be satisfied for all of them;

$$1 - P_{f_i} = [1 - P_1(\sigma_{N_i})]^{N_{eq_i}}, \quad N_{eq_i} = (D_i/l_0)\Psi_i, \qquad [9]$$

where $i = 1, 2, \ldots, n_k$. In each case, the stress in the weakest element, $\sigma = \sigma_{N_i}$ corresponds to the kink point, and in all of the other elements the stress is within the Weibull tail. Therefore, $P_1(\sigma_{N_i}) = r_0(\sigma_{N_i}/s_0)^m (i = 1, \ldots, n_k)$. Substituting this expression into the foregoing equation, one gets a system of equations. Considering only two cases ($n_k = 2$), there are two equations. Upon elimination of l_0

$$\frac{\ln(1 - P_{f_1})}{\ln(1 - P_{f_2})} = \frac{D_1\Psi_1 \ln[1 - r_f(\sigma_{N_1}/s_0)^m]}{D_2\Psi_2 \ln[1 - r_f(\sigma_{N_2}/s_0)^m]}, \qquad [10]$$

where r_f (close to 1) is known. This is a nonlinear equation, from which s_0 can be solved by Newton iterations, and l_0 then follows from Eq. **9**. Alternatively, one may eliminate s_0, and (if $n_k = 2$) this yields for l_0 the nonlinear equation

$$\frac{1 - (1 - P_{f_1})^{l_0/D_1\Psi_1}}{1 - (1 - P_{f_2})^{l_0/D_2\Psi_2}} = \left(\frac{\sigma_{N_1}}{\sigma_{N_2}}\right)^m, \qquad [11]$$

from which l_0 can be solved by Newton iterations; s_0 then follows from Eq. **9**. The grafting point probability for one RVE is then obtained as $P_{gr} = r_f(\sigma_{N_i}/s_0)^m$ for any i.

Preferably, the number of observations of the kink point should exceed two, and then the optimal values of l_0 and P_{gr} ensue by least-square nonlinear optimization of fit. Were the coefficient of variation from such regression too large, it would disprove the present theory.

Experimental Evidence from Histograms

Strength histograms with kink point on the Weibull scale plot were observed by Weibull (6) in his tests of Portland cement mortar (Fig. 3 *c* and *d*). The solid lines in Fig. 3 show that the present theory allows excellent fit. Lacking information, one may logically assume that $N_{eq} \approx 100$–$10{,}000$, and then the fitting of these data yields $P_{1gr} = 0.0001$–0.01 and $l_0 = 0.6$–1.0 cm.

However, Weibull (6) and all of the subsequent investigators up to now who observed similar kinked histograms for coarse-grained ceramics or very small material specimens have tried to deal with the kink points within the realm of the classical Weibull theory (for which the RVE size is 0). They noted that the optimum fits of these experimental histograms by Weibull distribution improve if one assumes a finite threshold σ_u (see Fig. 3*d*), i.e., if the tail is $P_1 = (\sigma - \sigma_u)^m/s_0^m$. On this basis, it has been widely claimed that some ceramics and fiber composites exhibit finite thresholds. However, the upper part of cdf could never be fitted.

According to the present analysis, these claims cannot be correct. The threshold must be zero, and, if the finite RVE size is taken into account, this finding leads to a much better fit of experimental strength histograms (Fig. 3*d*). This observation is of crucial importance for assessing loads of extremely small failure probabilities such as 10^{-6} to 10^{-7}. It is equally important for correct approach to the statistics of material strength on approach to nanoscale (MEMS, thin films, and nanocomposites).

Mean Size Effect Curve

Knowing the pdf, $p_1(\sigma_N)$, of one RVE, we can compute the mean σ_N (Fig. 3*b*) as $\bar{\sigma}_N = \int_0^\infty \sigma_N N_{eq}[1 - P_1(\sigma_N)]^{N_{eq}-1} p_1(\sigma_N) d\sigma_N$. Numerical integration yields, for geometrically similar structures, the mean size effect curve shown in Fig. 3*b*. Note that with decreasing size D the curve deviates from the power-law size effect of Weibull theory [the same also follows from deterministic energetic arguments (5, 34–36) emanating from ref. 37]. The onset of deviation is governed by P_{gr}, and the steepness of deviation is proportional to the coefficient of variation of RVE strength. If these two characteristics of the deviation from the power-law scaling of mean σ_N are identified experimentally, l_0 and P_{gr} can be evaluated. Agreement with the l_0 and P_{gr} values identified from kinks on experimental histograms verifies the theory.

When the mean size effect curve is fitted by the asymptotic matching formula for mean type I size effect (36, 38), the match is visually perfect (Fig. 3*b*). That formula, originally derived by energy arguments of fracture mechanics (34–36), was in turn shown to fit closely the size effect tests of mean flexural strength of various concretes and polymer–fiber composites collected from the literature (Fig. 3*b*) and also to agree closely with finite element simulations based on the nonlocal Weibull theory (39). These agreements support the present theory. Fitting both the mean size effect and the experimental histograms with their kink points provides a valuable check.

Conclusions and Implications

(*i*) In the case of quasibrittle structures, the safety (or understrength) factors used in design and the expected (mean) design strength cannot be considered as size independent. They both depend on the structure size (and shape) as measured by N_{eq}; this finding applies to concrete structures; to fiber composite parts of aircraft, ships, spacecraft and machines; and to rigid foams, tough ceramics, strengthening of seismically damaged structures by bonded laminates, etc.

(*ii*) Assessment of risk from landslides, avalanches, rock slides, tunnel or mining stope breakouts, or sea ice breaks should take into account the effect of size on both the mean strength and pdf type.

(*iii*) So should the failure analysis of MEMS, thin films, and nanocomposites, as well as quasibrittle biomaterials and bioinspired materials, etc.

(*iv*) The statistical fracture parameters of these materials can be identified by testing the strength histograms or the mean size effect on strength (or, better, both).

(*v*) The far-left tail of strength of any material must be a power law with zero threshold, although for plastic materials the tail lies so far away that it has no effect.

(*vi*) The power-law nature of pdf tail and Weibull pdf of large enough structures are an inevitable consequence of Maxwell–Boltzmann distribution of atomic energies and the stress dependence of activation energy.

(*vii*) The pdf of strength should be considered to depend on temperature and load duration or rate (as well as any corrosive agents that alter the activation energy barriers).

(*viii*) For predicting the failure of large quasibrittle structures, the RVE cannot be defined by homogenization.

Related Studies

Finally, it needs to be acknowledged that some aspects of the present model are partly related to important probabilistic models of the lifetime distribution and of the evolution of defects in parallel coupling systems with various idealized load-sharing and interaction rules (e.g., refs. 40–45 and references therein). Like the present model, the lifetime modeling, too, has been physically justified by the stress dependence of activation energy, through an argument traced to Eyring (46, 47), similar to that underlying Eq. **1**.

Remarks on Nanotubes, Etc.

According to the hierarchical model in Fig. 2*e*, the left-tail power-law exponent m can be as small as 1–4 for nanotubes, thin films, and various long nanometer-width components. The resulting statistical size effect would be much stonger than in standard material tests, e.g., $\sigma_N \propto D^{-1/2}$ to D^{-1}. Creating parallel connections, such as cross-linking in multiple nanotubes or nanotube bundles, would mitigate this size effect.

This work was supported by Office of Naval Research Grant N00014-10-I-0622 (to Northwestern University), National Science Foundation Grant CMS-0556323 (to Northwestern University), and a Department of Transportation grant (to the Infrastructure Technology Institute at Northwestern University).

1. Duckett, W. (2005) *Struct. Engineer* **15,** 25–26.
2. Melchers, R .E. (1987) *Structural Reliability, Analysis & Prediction* (Wiley, New York).
3. Rubeša, D., Smoljan, B. & Danzer, R. (2005) *J. Mater. Eng. Perform.* **12,** 220–228.
4. Bažant, Z. P. & Pang, S.-D. (2006) *J. Mech. Phys. Solids* **54,** in press.
5. Bažant, Z. P. & Planas, J. (1998) *Fracture and Size Effect in Concrete and Other Quasibrittle Materials* (CRC, Boca Raton, FL).
6. Weibull, W. (1939) *Proc. R. Swedish Inst. Eng. Res.* **153,** 1–55.
7. Freudenthal, A. M. (1968) in *Fracture: An Advanced Treatise*, ed. Liebowitz, H. (Academic, New York), Vol. 2, pp. 591–619.
8. Curtin, W. A. & Scher, H. (1991) *Phys. Rev. B Condens. Matter* **45,** 2620–2627.
9. Mayer, J. E. (1940) *Statistical Mechanics* (Wiley, New York).
10. McClintock, A. M. & Argon, A. S. (1966) *Mechanical Behavior of Materials* (Addison–Wesley, Reading, MA).
11. Hill, T. L. (1960) *An Introduction to Statistical Mechanics* (Addison–Wesley, Reading, MA).
12. Cottrell, A. H. (1964) *The Mechanical Properties of Matter* (Wiley, New York).
13. Glasstone, S., Laidler, K. J. & Eyring, H. (1941) *The Theory of Rate Processes* (McGraw–Hill, New York).
14. Daniels, H. E. (1945) *Proc. R. Soc. London Ser. A* **183,** 405–435.

15. Feller, W. (1957) *Introduction to Probability Theory and its Applications* (Wiley, New York).
16. Harlow, D .G., Smith, R. L. & Taylor, H. M. (1983) *J. Appl. Probability* **20,** 358–367.
17. Harlow, D. G. & Phoenix, S. L. (1978) *J. Composite Mater.* **12,** 195–334.
18. Mahesh, S., Phoenix, S. L. & Beyerlein, I. J. (2002) *Int. J. Fracture* **115,** 41–85.
19. Phoenix, S. L. & Beyerlein, I. J. (2000) *Phys. Rev. E* **62,** 1622–1645.
20. Bansal, G. K., Duckworth, W. H. & Niesz, D. E. (1976) *J. Am. Ceramic Soc.* **59,** 472–478.
21. Ito, S., Sakai, S. & Ito, M. (1981) *Zairyo* **30,** 1019–1024.
22. Katayama, Y. & Hattori, Y. (1982) *J. Am. Ceramic Soc.* **65,** C-164–C-165.
23. Matsusue, K., Takahara, K. & Hashimoto, R. (1982) *Yoyo Kyokaishi* **90,** 168–174.
24. Quinn, G. D. & Morrell, R. (1991) *J. Am. Ceramic Soc.* **74,** 2037–2066.
25. Katz, R. N., Wechsler, G., Toutjanjim, H., Friel, D., Leatherman, G. L., El-Korchi, T. & Rafaniello, W. (1993) *Ceramic Eng. Sci. Proc.* **14,** 282–291.
26. Danzer, R. & Lube, T. (1996) in *Fracture Mechanics of Ceramics*, eds. Bradt, R. C., Hasselmann, D. P. H., Munz, D., Sakai, M. & Yu Shevchenkov, V. (Plenum, New York), pp. 425–439.
27. Santos, C., Strecker, K., Neto, F. P., Silva, O. M. M., Baldacim, S. A. & Silva, C. R. M. (2003) *Mater. Res.* **6,** 463–467.
28. Lu, C., Danzer, R. & Fischer, F. D. (2002) *Phy. Rev. E* **65,** 067102-1–067102-4.
29. Julian, O. G. (1955) *Am. Concrete Inst. Proc.* **51,** 772–778.
30. Shalon, R. & Reintz, R. C. (1955) *Proceedings of the Réunion Internationale des Laboratoires d'Essais et de Recherches sur les Matériaux et les Constructions Symposium on the Observation of Sub-structures* (Réunion Internationale des Laboratoires d'Essais et de Recherches sur les Matériaux et les Constructions, Lisbon, Portugal), Vol. 2, pp. 100–116.
31. Rüsch, H., Sell, R. & Rackwitz, R. (1969) *Deutscher Ausschuss für Stahlbeton*, German Committee for Reinforced Concrete (Ernst & Sohn, Berlin), No. 206.
32. Mirza, S. A., Hatzinikolas, M. & MacGregor, J. G. (1979) *J. Struct. Div. ASCE* **105,** 1021–1037.
33. Chmielewski, T. & Konopka, E. (1999) *Magn. Concrete Res.* **51,** 45–52.
34. Bažant, Z. P. & Chen, E.-P. (1997) *Appl. Mech. Rev. ASME* **50,** 593–627.
35. Bažant, Z. P. (2005) *Scaling of Structural Strength* (Elsevier, London).
36. Bažant, Z. P. (2004) *Proc. Natl. Acad. Sci. USA* **101,** 13397–13399.
37. Bažant, Z. P. (1984) *J. Eng. Mech. ASCE* **110,** 518–535.
38. Bažant, Z. P. (2004) *Prob. Eng. Mech.* **19,** 307–319.
39. Bažant, Z. P. & Xi, Y. (1991) *J. Eng. Mech. ASCE* **117,** 2623–2640.
40. Phoenix, S. L. (1978) *SIAM J. Appl. Math.* **34,** 227–246.
41. Phoenix, S. L. & Tierney, L.-J. (1983) *Eng. Fracture Mech.* **18,** 193–215.
42. Newman, W. I. & Phoenix, S. L. (2001) *Phys. Rev. E* **63,** 021507-1–012507-20.
43. Curtin, W. A. & Scher, H. (1997) *Phys. Rev. B Condens. Matter* **55,** 12038–12050.
44. Phoenix, S. L., Ibnabdeljalil, M. & Hui, C.-Y. (1997) *Int. J. Solids Struct.* **34,** 545–568.
45. Phoenix, S. L. & Smith, R. L. (1983) *Int. J. Solids Struct.* **19,** 479–496.
46. Eyring, H. (1936) *J. Chem. Phys.* **4,** 283–291.
47. Tobolsky, A. V. (1960) *Structure and Properties of Polymers* (Wiley, New York).